Eur. J. Mineral.
2006, **18**, 641-651

Fine-probing the crystal-chemistry of talc by MAS-NMR spectroscopy

François MARTIN[1, 2]*, Eric FERRAGE[3], Sabine PETIT[4], Philippe de PARSEVAL[2], Luc DELMOTTE[5], Jocelyne FERRET[6], Didier ARSEGUEL[6] and Stefano SALVI[2]

[1]HydrASA, UMR 6532 Université de Limoges-CNRS, 123 avenue Albert Thomas, F-87060 Limoges, France
[2]ERT Géomatériaux et HYMEDIA, UMR 5563 Université Paul Sabatier-CNRS, OMP-LMTG,
14 avenue Edouard Belin, F-1000 Toulouse, France
[3]Department of Mineralogy, The Natural History Museum, Cromwell Road, London, SW7 5BD, UK
[4]HydrASA, UMR 6532 Université de Poitiers-CNRS, 40 avenue du Recteur Pineau, F-86022 Poitiers Cedex, France
[5]Laboratoire de Matériaux à Porosité Contrôlée, UMR 7016 Université de Mulhouse-CNRS, ENSCMu,
3 rue Alfred Werner, F-68093 Mulhouse Cedex, France
6 Talc de Luzenac S.A., BP 1162, F-31036 Toulouse Cedex, France

Abstract: Magic-Angle-Spinning Nuclear Magnetic Resonance (MAS-NMR) spectroscopy was used to probe the crystallographic environment of Si, Al, F and H in 14 natural talc samples originating from different localities and containing various, small amounts of iron ($Fe_2O_{3\ [total]} < 2$ wt %). We show that iron induces strong variations in NMR spectra and that even very low quantities can be used as an indirect NMR parameter to characterize in detail the crystal-chemistry of talc. Conversely, their correlations with full width at half height (FWHH) in MAS-NMR spectra for ^{29}Si, ^{27}Al, ^{1}H, and ^{19}F obtained from these 14 talc samples allow for rapid estimations of the total iron content. Finally we highlight how, by simply recording Mössbauer, NIR and NMR spectra, one can obtain an accurate structural formula of talc, which is a necessary parameter for uses in specific industrial applications.

Key-words: MAS-NMR, talc, crystal-chemistry, substitution, iron.

1. Introduction

Talc ($Si_4Mg_3O_{10}(OH)_2$), the magnesium end-member of the 2:1 phyllosilicates family, has very limited tetrahedral and octahedral element substitutions and, as a result, it has a layer charge of zero and an atom-free interlayer space (Martin *et al*., 1999). This "ideal" crystal chemistry, added to properties such as lamellar particle shape and lubricant characteristics, confer to talc a wide range of industrial applications, ranging from the ceramic to cosmetic industries, paint and paper manufacturing, and polymer engineering. In the latter application talc is used as filler, thereby inducing an increase in crystallization temperature and improving the mechanical properties of the various composites (Menczel & Varga, 1983; Gonzalez *et al*., 1995; Tiganis *et al*., 1996; Ferrage *et al*., 2002). Recently, the crystal chemistry of talc has been refined by Martin *et al*. (1996, 1999) and Petit *et al*. (2004a and b) who used spectroscopic methods to confirm the potential of talc to incorporate only small amounts of cations (*e.g.*, Al and Fe^{3+}) and anions (*e.g.*, F-) in both tetrahedral and octahedral sheets. They also indicated that Fe^{2+} and Mn were found only in octahedrally coordinated sites, and that such substitutions could induce local modifications of the surface properties of the mineral. In addition, Ferrage *et al.* (2002) have stressed the importance of the talc-polymer interface in determining the properties of the final compound. It is therefore evident that a more accurate determination of the crystal chemistry of talc could have important implications for the industrial applications of this mineral species.

In this paper we make use of Magic Angle Spinning-Nuclear Magnetic Resonance (MAS-NMR) spectroscopy to investigate the crystallographic environment of Si, Al, F and H in talc, using 14 natural talc samples from various localities. The efficiency of the technique is assessed by locally probing the nature of the cations and their distribution in the different crystallographic sites.

1.1. NMR information on Fe (and Mn) cationic presence in phyllosilicates

It is well established that solid-state ^{29}Si and ^{27}Al NMR spectroscopy is an essential tool in investigating the short-range order and structural configuration of aluminosilicates, such as tetrahedral $^{[4]}Al$ and octahedral $^{[6]}Al$ distribution, and the distribution of paramagnetic impurities (Sanz & Serratosa, 1984; Barron *et al*., 1985a and b;

*E-mail: francois.martin@unilim.fr

DOI: 10.1127/0935-1221/2006/0018-0641
0935-1221/06/0018-0641 $ 4.95

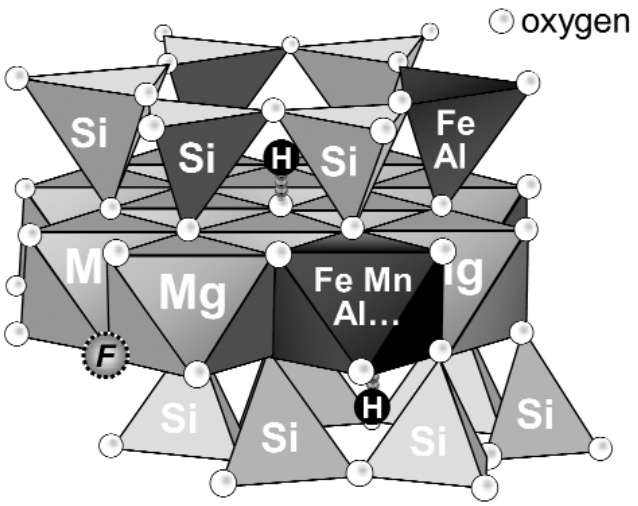

Fig. 1. Details of the structure of talc (2:1 phyllosilicate) showing the possible cation substitutions in tetrahedral (silicon (Si) by aluminium (Al) and/or iron (Fe^{3+})), and/or octahedral (magnesium (Mg) by manganese (Mn) and/or aluminium (Al) and/or iron (Fe^{3+}, Fe^{2+})) sites and the replacement of hydroxyl groups (OH-) by fluor (F) anions.

Kinsey *et al*., 1985; Altaner *et al*., 1987; Herrero *et al*., 1987, Herrero & Sanz, 1991; Sanz & Robert, 1992; Rocha & Pedrosa de Jesus, 1994; Welch *et al*., 1995; Schroeder & Pruett, 1996; Kentgens, 1997; Dékany *et al*., 1999; Lausen *et al*., 1999; Sainz-Diaz *et al*., 2001; d'Espinosse de la Callerie *et al.*, 2002). However, it has been shown that the presence of ferromagnetic impurities (Fe, Mn, …) can cause severe peak broadening, in particular in natural samples (Grimmer *et al*., 1983; Oldfield *et al.*, 1983; Morris *et al.*, 1990). In the worst scenarios, peaks can be so broadened to become undetectable. This deformation is caused by several chemical shifts, which are themselves due to the interaction of unpaired *d* or *f* electrons with the nucleus. Although the problem of peak broadening is well known, this issue has never been systematically investigated up to now. In general, it appears that phases containing major Fe or Mn cannot be observed by NMR, and that as little as 1 to 2 wt.% oxides, although they do not totally destroy the spectrum, can cause sufficient peak broadening to result in very poor resolution (at least for ^{29}Si) (Altaner *et al*., 1987). These paramagnetic effects may be less important for quadrupolar nuclides with intrinsically broad peaks. Also, Fe^{2+} should have a larger peak broadening effect than Fe^{3+}, simply because Fe^{2+} has more unpaired *d*-electrons (Palinko *et al*., 1996). Iron causes rapid relaxation of all the Si sites and small amounts can give rise to low signal-to-noise ratios (Altaner *et al*., 1987). Therefore, the presence of paramagnetic Fe^{3+} ions makes the NMR resonance of a significant fraction of the ^{29}Si signal broadened beyond detection. However, this broadening occurs only if the distance among iron and silicon atoms is not great (Bruni *et al*., 1999). The NMR relaxation theory for systems containing paramagnetic centres describes the interaction between a paramagnetic centre and nearby lattice nuclei. Thus, following this approach, one could obtain structural and dynamical information from NMR relaxation experiments. The radius of paramagnetic interactions that can be detected in a single Fe^{3+} is about 5 nm (Purcell *et al*., 1948). The resulting ^{27}Al NMR signal intensity depends on the effective Fe wipeout-sphere radius, which Schroeder & Pruett (1996) bracketed between 6 and 10 Å. Cuadros *et al.* (1999) tested different effective radii (in the range of 6 to 8.5 Å) and found a minimum value of 7.5 Å. It follows that the total NMR signal from octahedral Al depends on the amount of octahedral Fe and its distribution. Increasing Fe segregation causes higher ^{27}Al NMR intensity because less Al atoms are close enough to Fe atoms for their NMR signal to be lost. Knowing the octahedral Fe and Al content in a sample, together with the corresponding octahedral Al NMR signal intensity, allows the indirect evaluation of how Fe is distributed in the octahedral sheet of phyllosilicates (Schroeder, 1993).

1.2. NMR information on Si, Al and Si-Al cationic environments in phyllosilicates

Lippmaa *et al*. (1980 and 1981) originally demonstrated that the ^{29}Si chemical shift in solid silicates is sensitive to both the degree of condensation of SiO_4 units, single or double chain, sheet or framework, and the chemistry of the second coordination sphere. Within the tetrahedral sheets of the 2:1 phyllosilicates, tetrahedral SiO units are in a Q^3 environment, *i.e.*, bonded to three other tetrahedral units. It has been shown that the degree of condensation of SiO_4 units significantly affects the ^{29}Si chemical shift, with Q^3 units resonating in the range of –90 ppm to –100 ppm. The ^{29}Si MAS-NMR spectra of talc and pyrophyllite show a single component that appears at –97 ppm for talc and at –94 ppm for pyrophyllite. The difference in chemical shift is a consequence of differences in composition of the octahedral sheet. On the other hand, each octahedron shares edges with six adjacent octahedra and also shares oxygens with four tetrahedra, two on each side of the octahedral sheet. The effect that those second neighbours (located in different sites of the structure, *e.g.*, tetrahedral or octahedral sheets, and, only for micas and smectites, interlayer space), exert on the chemical shift of the Si and Al signals can be analysed separately by comparing sample pairs with appropriate compositions (Sanz & Serratosa, 1984; Engelhardt & Michel, 1987; Plévert *et al.*, 2001).

In the dioctahedral phyllosilicates (pyrophyllite, muscovite and margarite) $^{[6]}$Al lines appear at about 1-2 ppm. In trioctahedral mineral containing small amounts of Al in the octahedral sheet each Al ion must be surrounded by six Mg ions and the $^{[6]}$Al line appears at 5-6 ppm. This value is higher than those observed for dioctahedral minerals where each Al ion is surrounded by three Al and three vacancies. Generally, clay minerals contain $^{[4]}$Al and $^{[6]}$Al and the ^{27}Al MAS-NMR spectra consist of one or two principal components plus a series of sidebands associated to the spinning of the samples. The central line at 0 ppm is assigned to octahedral Al ions whereas the line at 70 ppm to tetrahedral Al ions. In all cases, the $^{[4]}$Al signal shows a

greater half-width than the $^{[6]}$Al one. In principle, a quantitative determination of $^{[4]}$Al/$^{[6]}$Al ratio appears possible with high-resolution spectra but requires higher magnetic fields than that used in this work (94 kG) to eliminate the second-order quadrupolar effects.

1.3. NMR information on H environments in phyllosilicates

Solid-state proton NMR offers an extremely useful tool in the characterization of structural hydroxyls and water, as well as adsorbed molecules. In particular, the chemical shifts are characteristic of the hydrogen environment, whereby different bands are associated to different structural sites (Alba *et al*., 2000 and 2001; Di Leo & Cuadros, 2003). We can expect the presence of only one peak in MAS-NMR spectra for talc and symmetry of the spinning sideband pattern, due to H location in the hexagonal ring (Fig. 1). This structural hydrogen can be influenced directly by tetrahedral and octahedral substitutions (Martin *et al*., 1996). Trioctahedral micas with high Fe contents can experience splitting of the ^{1}H NMR hydroxyl-proton, due to Fe location in different neighbouring octahedral positions (Sanz, 1990). However, this effect should be negligible in our study due to the relatively low Fe content.

2. Samples and experimental procedure

2.1. Samples

The talc samples used in this paper have been previously studied by NIR (near infrared) and FTIR spectroscopy (Petit *et al*., 2004a and b). Sample origin, locality, and electron-microprobe analyses are provided in Table 1. All samples consist entirely of pure talc, apart from sample 11, which contains traces of a 7 Å phase (*i.e.*, a 1:1 phyllosilicate-type mineral). Structural formulae were calculated from microprobe analyses on the basis of 11 oxygen equivalents (Petit *et al*., 2004a and b) and are listed in Table 2. The atomic distributions of iron and aluminium were derived from Mössbauer and NMR measurements, respectively. As shown in Tables 1 and 2, the samples display a wide range of Fe, Al, and F contents (up to 0.1, 0.34, and 0.29 atom per half unit-cell, respectively).

2.2. Nuclear Magnetic Resonance Spectroscopy

Solid-state NMR experiments were performed as follows: ^{29}Si NMR measurements were carried out on a Bruker MSL-300 spectrometer operating at B_0 = 7.1 T (ν_0 = 59.63 MHz). The ^{27}Al , ^{1}H and ^{19}F NMR spectra were collected on a Bruker DSX-400 spectrometer operating at B_0 = 9.4 T (ν_0 = 104.263 MHz, ν_0 = 400.13 MHz and ν_0 = 376.49 MHz). Single-pulse magic-angle spinning spectra were obtained on a Bruker MAS probe, with a 7-mm ZrO_2 rotor for ^{29}Si experiment and a 4-mm rotor for ^{27}Al and ^{19}F. Acquisitions parameters are summarized in Table 3. The ^{29}Si, ^{27}Al and ^{19}F chemical shifts were referenced externally to TMS (tetramethylsilane), aqueous $Al(H_2O)_6^{3+}$, and $CFCl_3$ (trichlorofluoromethane), respectively.

NMR spectra decomposition was performed by least-square fitting and mixed Lorentzian-Gaussian shapes functions (1% < Gaussian < 5%), using the GRAMS/AI (ver. 7.01) software from Thermo Galactic. A linear baseline was considered systematically, and fit progress was monitored by successive iterations until a good quality of reproduction was obtained. Selected results of the fitting procedure are illustrated in Fig. 2a, b, c and d for ^{29}Si, ^{27}Al, ^{1}H, and ^{19}F, respectively. The widths of the Lorentzian curves discussed in the following refer to the full width at

Table 1. Chemical analyses as determined by electron microprobe, and origin of the talc samples.

						%				
Sample	SiO_2	Al_2O_3	Fe_2O_3	MgO	NiO	CaO	K_2O	Na_2O	TiO_2	F
(1) Brazil Fourty, Brazil, originating from ultrabasic rocks										
	63.02	0.02	2.07	29.71	0.00	0.01	0.01	0.01	0.01	0.03
(2) Val Chizone, Italy, originating from dolomite alteration										
			1.71							
(3) Rabenwald, Austria, originating from magnesite alteration (Moine *et al.,* 1989)										
	62.32	0.24	0.92	30.04	0.00	0.00	0.03	0.02	0.00	0.25
(4), (5) T111, Trimouns, France, originating from dolomite alteration (Moine *et al.,* 1989; Martin *et al.,* 1999; Schärer *et al.,* 1999)										
	61.67	0.19	0.68	31.52	0.00	0.02	0.00	0.00	0.00	0.16
(6) Roc Martin, Afghanistan, originating from high grade metamorphism talcschist (Kulke & Schreyer, 1973)										
	56.71	4.31	0.48	28.24	0.00	0.02	0	0.91	0.28	0.3
(7) and (8) Guangxi, China, originating from dolomite alteration										
	62.72	0.03	0.45	30.77	0.00	0.01	0.01	0.02	0.01	0.19
(9) and (10) Set 16, Leon, Spain, originating from dolomite alteration (Galan-Huertos & Rodas, 1973)										
	62.19	0.17	0.16	32.37	0.00	0.00	0.00	0.04	0.00	1.00
(11) Gabon, originating from carbonate alteration										
	62.99	0.07	0.07	30.85	0.00	0.05	0.02	0.21	0.00	1.44
(12) Pink Haïcheng, China, originating from magnesites alteration										
	63.19	0.00	0.06	32.08	0.00	0.05	0.05	0.07	0.02	0.00
(13) and (14) Liaoyong White, China, originating from magnesites alteration										
	64.01	0.036	0.04	31.46	0.00	0.02	0.01	0.06	0.00	0.30

Samples 2, 3, 4, 5, 9, 10, 12, 13 and 14 are from the collection of Talc Luzenac Europe; samples 1, 6, 7, 8 and 11 are from F. Martin's collection.

Table 2. Structural formulae of talc samples calculated based on 11 oxygen equivalents.

Samples	1	2	3	4	6	7 and 8	9 and 10	11	12	13 and 14
Si	4		4.01	3.96	3.79	4.02	3.99	4.02	3.99	4.02
Al	0.002		0.018	0.014	0.34	0.002	0.020	0.005	0.000	0.003
Fe	0.10		0.044	0.037	0.024	0.021	0.009	0.003	0.003	0.003
Mg	2.84		2.89	3.02	2.81	2.94	2.99	2.94	3.02	2.95
Ni	0.00		0.00	0.00	0.00	0.00	0.00	0.00	0.00	0.00
Ti	0.00		0.00	0.00	0.01	0.00	0.00	0.00	0.00	0.00
F	0.01		0.05	0.05	0.06	0.04	0.2	0.29	0	0.06
OH	1.99		1.95	1.95	1.94	1.96	1.8	1.71	2	1.94
% [6] Fe^{2+}	53		78	68	60	85	60	-	-	-
% [6] Fe^{3+}	14		0	18	30	5	0	-	-	-
% [4] Fe^{3+}	33		22	14	10	10	40	-	-	-
% [6] Al	64	76	35	51	81	34	0	86	-	61
% [4] Al	36	24	65	49	19	66	100	14	-	39

The iron and aluminium atomic distributions are from Mössbauer and NMR measurements. - indicates not measured.

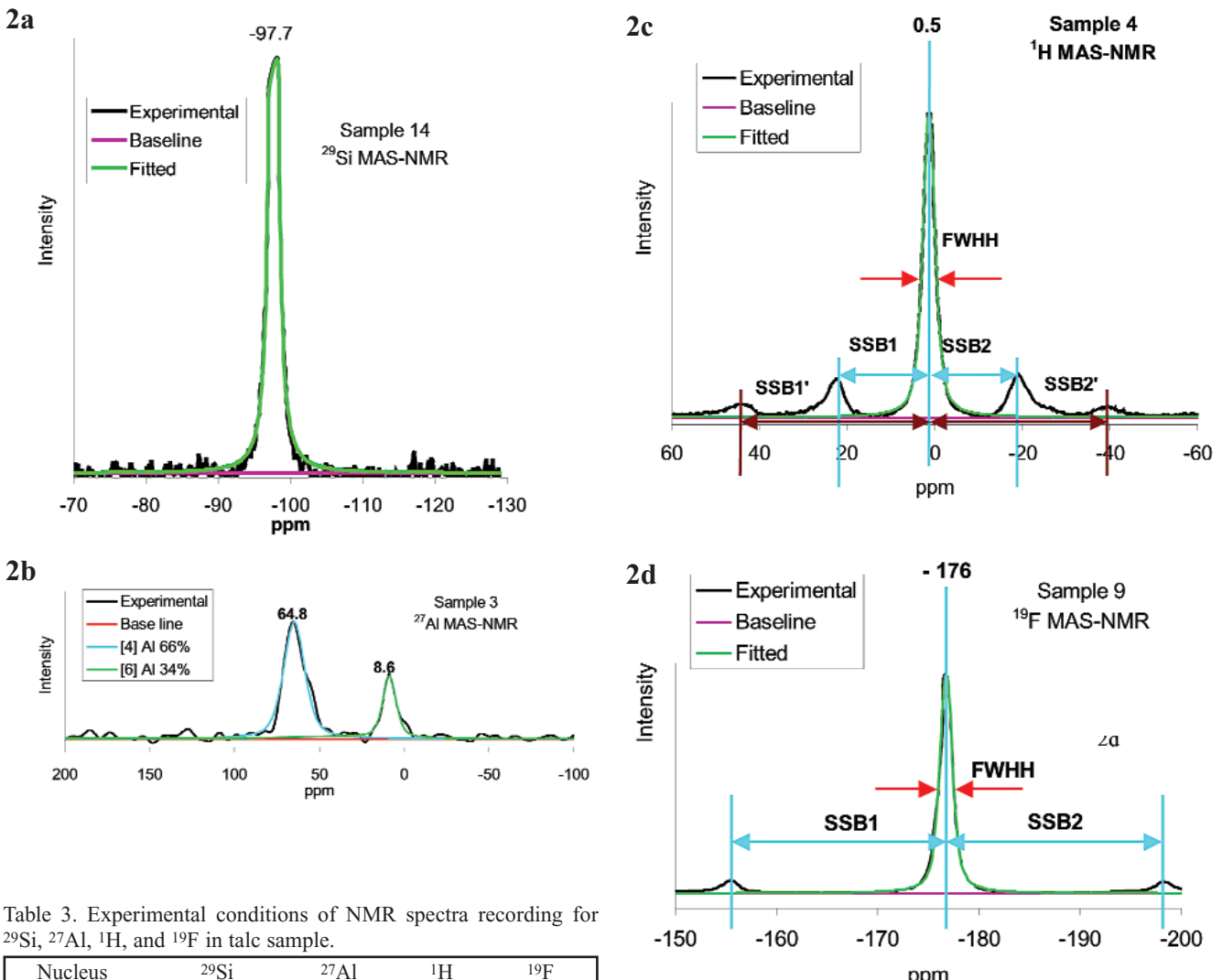

Table 3. Experimental conditions of NMR spectra recording for ^{29}Si, ^{27}Al, ^{1}H, and ^{19}F in talc sample.

Nucleus	^{29}Si	^{27}Al	^{1}H	^{19}F
Spinning speed (kHz)	4	10	8	12
Pulse length (flip angle)	3.25 µs (π/4)	1 µs (π/12)	3 µs	3.6 µs (π/2)
Recycle delay	2 mn	1 s	20 s	10 s

Fig. 2. Solid state MAS-NMR spectra recorded on natural talc samples. (a) ^{29}Si (sample 4), (b) ^{27}Al (sample 3), (c) ^{1}H (sample 4), and (d) ^{19}F (sample 9). An example of the decomposition process in quasi-Lorentzian elementary contributions is illustrated for each element (green line), SSB indicates spinning sidebands whereas FWHH refers to the full width at half heights.

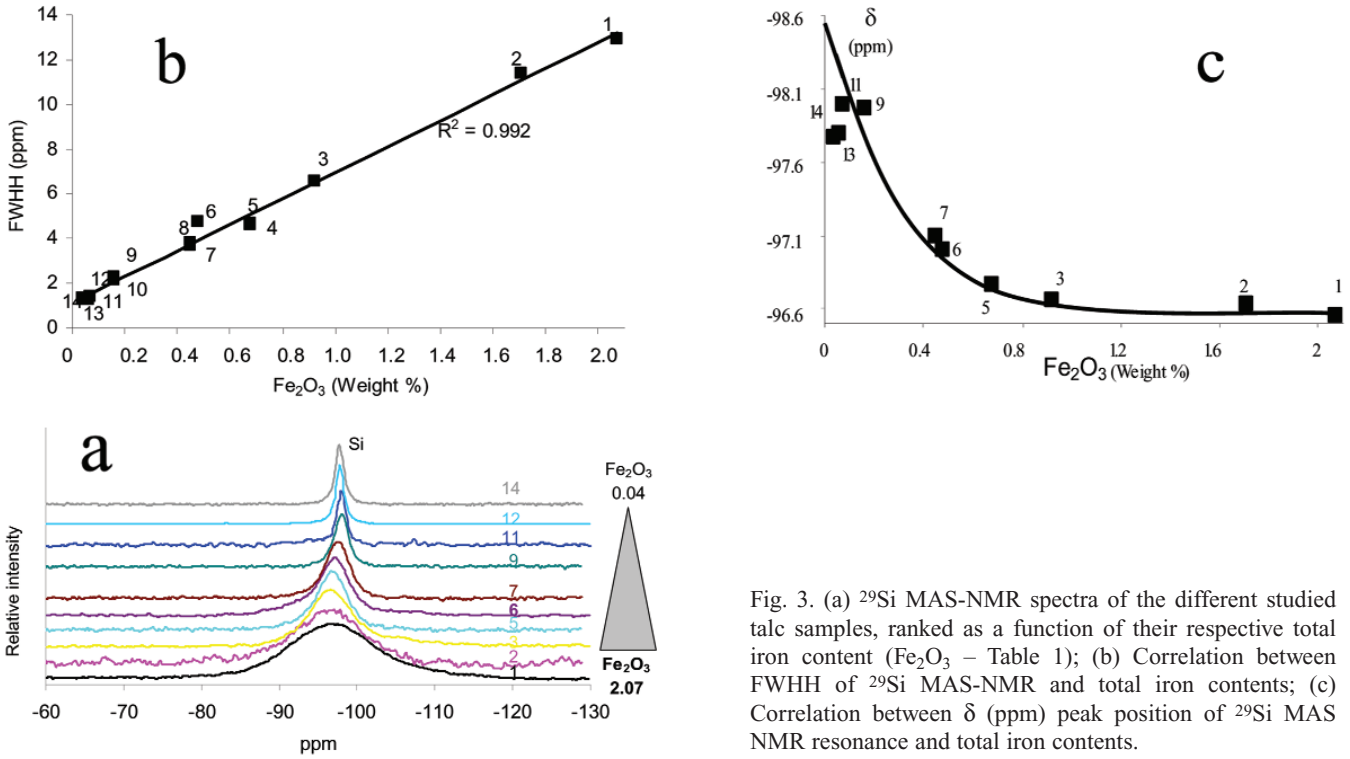

Fig. 3. (a) ^{29}Si MAS-NMR spectra of the different studied talc samples, ranked as a function of their respective total iron content (Fe_2O_3 – Table 1); (b) Correlation between FWHH of ^{29}Si MAS-NMR and total iron contents; (c) Correlation between δ (ppm) peak position of ^{29}Si MAS NMR resonance and total iron contents.

half height (FWHH). Spinning sidebands are referred to as SSB in Fig. 2c and d.

3. Results

3.1 General features of talc multinuclear MAS-NMR spectra

The ^{29}Si shift is influenced strongly by the chemical environment of the silicon nucleus and is highly correlated with the degree of SiO_4 tetrahedra polymerization, notably, with the amount of next-near-neighbour Al atoms (Lippmaa *et al*., 1980, 1981; Mägi *et al*., 1984; Kinsey *et al*., 1985; Kirkpatrick, 1988). The ^{29}Si MAS-NMR spectrum for talc typically shows an asymmetrical peak around –98 ppm, which is attributed to Q^3 species (Lippmaa *et al*., 1980, 1981) and is characteristic of clay minerals (Fig. 2a). No spinning sidebands were detected, indicating the absence of chemical shift anisotropy (Smith *et al*., 1983), but also the absence of different magnetic impurity types (Oldfield *et al*., 1983), as well as of visible dipolar interactions (Grimmer *et al*., 1983).

The ^{27}Al MAS-NMR spectrum allows one to differentiate readily and unambiguously between four- and six-fold-coordinated aluminium atoms because of well-separated positional shifts (Fig. 2b). According to Barron *et al*. (1985a and b) and Herrero *et al*. (1985a and b), the two resonances around 9 ppm and 64 ppm are classically attributed to Al in octahedral and tetrahedral sites, respectively. Integration of the area under each MAS-NMR peak provides semi-quantitative estimates of $^{[4]}$Al and $^{[6]}$Al amounts. However, this simple measurement is constrained to some selective conditions of excitation, such as using very short pulse width (0.7 µs) corresponding to a small flip angle of π/12. As for ^{29}Si, no spinning sidebands are detected for aluminium.

The ^{1}H MAS-NMR spectrum displays a band located around 0.5 ppm, which is characteristic of trioctahedral minerals (Oldfield *et al*., 1983; Welch *et al*., 1995; Alba *et al*., 2000; Di Leo & Cuadros, 2003 – Fig. 2c). The presence of a single central peak and the location and intensity symmetry of the spinning sidebands with respect to I (I_{SSB1} = I_{SSB2} and $I_{SSB1'}$ = $I_{SSB2'}$) indicate a single site for H with an isotropic environment (OH-bond axes being perpendicular to the layers and pointing toward the hexagonal cavities). Note that according to Oldfield *et al*. (1983), these spinning sidebands are induced by the presence of magnetic impurities.

The ^{19}F MAS-NMR spectrum for talc shown in Fig. 2d exhibits one resonance around -176 ppm, indicating the presence of a single type of structural site (Huve *et al*., 1992; Fyfe *et al*., 2001). Such signal has already been observed for trioctahedral 2:1 layer silicates and is commonly attributed to F atoms bonding to three Mg atoms (Mg-Mg-Mg environment) in an isotropic configuration (with SSB1 = SSB2).

3.2. Influence of total iron (Fe_2O_3) content on multinuclear MAS-NMR spectra

3.2.1. ^{29}Si

The ^{29}Si MAS-NMR spectra of our talc samples show similar single resonance at around –96 ppm and –98 ppm, which is consistent with Q^3 species (Lippmaa *et al*., 1980, 1981) (Fig. 3a). However, significant variations in FWHH

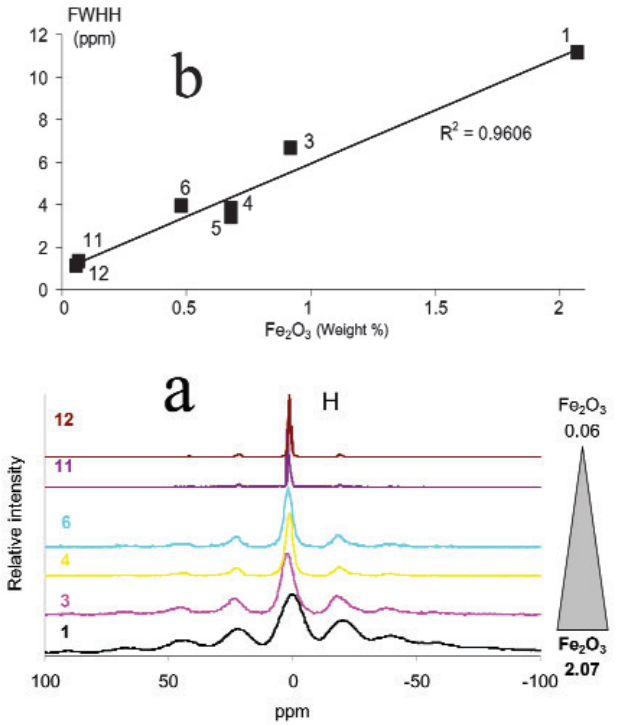

Fig. 4. (a) ^{1}H MAS-NMR spectra of the different talc samples, ranked as a function of their respective total iron content (Fe_2O_3 – Table 1); (b) Correlation between FWHH of ^{1}H MAS-NMR and total iron contents.

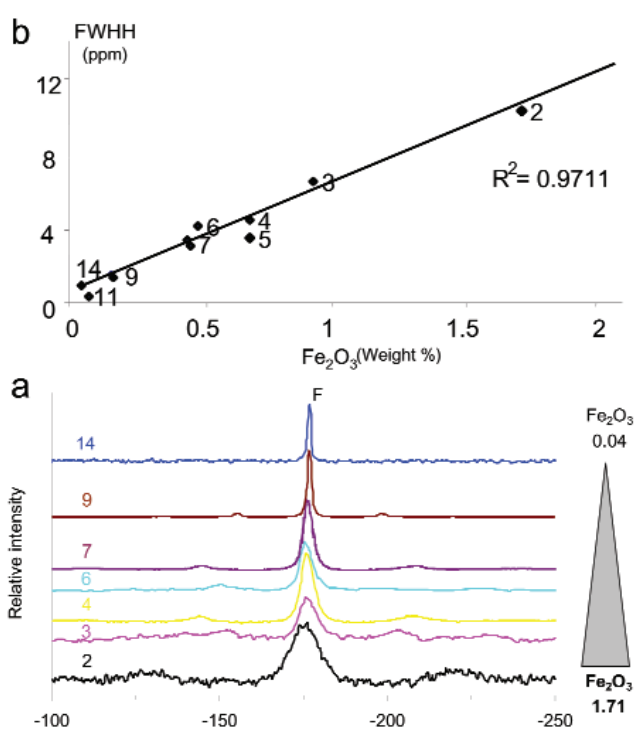

Fig. 5. (a) ^{19}F MAS-NMR spectra of the different talc samples, ranked as a function of their respective total iron content (Fe_2O_3 – Table 1); (b) Correlation between FWHH of ^{19}F MAS-NMR and total iron contents.

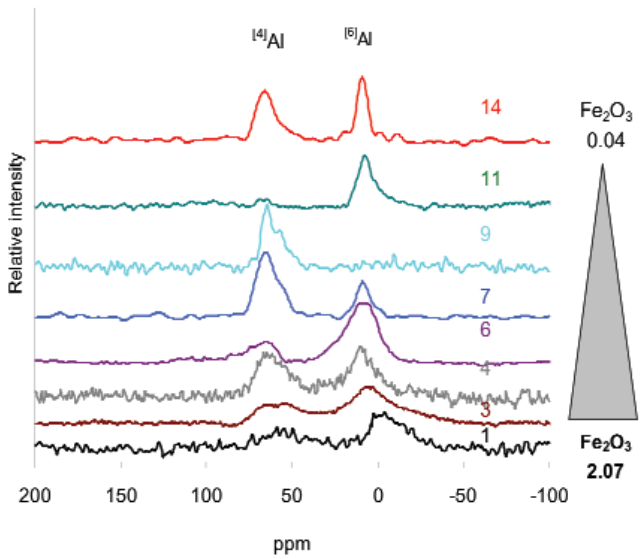

Fig. 6. ^{27}Al MAS-NMR spectra of the talc samples, ranked as a function of their respective total iron content (Fe_2O_3 – Table 1).

can also occur from 12.95 ppm to 1.24 ppm, as shown in Fig. 3a and 3b for samples 1 and 14, respectively. A possible explanation for this variation can be obtained by ranking the different ^{29}Si spectra as a function of their respective Fe_2O_3 content (total iron content – Fig. 3); indeed, the width of ^{29}Si resonance peaks increases with the iron content of the sample. Plotting ^{29}Si peak FWHH *vs.* Fe_2O_3 content results in a linear correlation (Fig. 3b) which yields the FWHH limit value for pure talc (no iron present), at about 0.5 ppm to 1 ppm. In addition, Fig. 3a also shows that the resonance peak position (δ) increases gradually in the –96 ppm to –98 ppm range with increasing Fe_2O_3 amount. A regression using a power function (Fig. 3c) yields the ideal ^{29}Si peak position for pure iron-free talc, which is close to –98.5 ppm. This limit differs from those measured by Lippmaa *et al*. (1980, 1981), Mägi *et al*. (1984), Kinsey *et al*. (1985), and Kirkpatrick (1988), most likely due to presence of very small amounts of iron in their sample.

3.2.2. ^{1}H

The ^{1}H MAS-NMR spectra also display some variation with total iron contents, namely, as for ^{29}Si, a decrease of FWHH with decreasing Fe_2O_3 content (Fig. 4a). In addition, the intensity and the asymmetric spinning sidebands decrease as the Fe_2O_3 content decreases (sample 12). For samples having high iron contents, spinning sidebands are more likely related to an increase in dipolar interactions (near octahedrally or tetrahedrally coordinated Fe atoms) from a contact term between the unpaired electrons of Fe centres and ^{1}H.

Similarly to ^{29}Si, a linear dependence is observed between Fe_2O_3 and ^{1}H MAS-NMR FWHH, leading to a FWHH limit value for pure iron-free talc of about 1 ppm

Table 4. Structural formulae of talc samples, calculated from NIR, Mössbauer, and chemical microprobe analyses taking into account NMR data for the distribution of $^{[6]}Al^{3+}$ and $^{[4]}Al^{3+}$.

	1	2	3	4 and 5	6	7 and 8	9 and 10	11	12	13 and 14
Si	3.84328		3.9513	3.97714	3.9314	3.99068	3.97	3.9993	4	3.99883
$^{[4]}Al$	0.00072		0.0117	0.00686	0.0646	0.00132	0.02	0.0007	0	0.00117
$^{[4]}Fe^{3+}$	0.156		0.037	0.016	0.004	0.008	0.010	—	—	—
	± 0.005		± 0.003	± 0.002	± 0.001	± 0.001	± 0.002			
Mg	2.749		2.809	2.914	2.705	2.918	2.985	3	2.996	3
Fe^{2+}			0.251	0.132	0.077	0.026	0.067	0.015	0	0.004
$^{[6]}Fe^{3+}$	0.066		0	0.020	0.013	0.004	0	—	—	—
	± 0.012			± 0.005	± 0.003	± 0.001				
$^{[6]}Al$	0.00128		0.0063	0.00714	0.2754	0.00068	0	0.0043	0	0.00183
Σ oct.	3.06728		2.9473	3.01814	3.0194	2.98968	3.000	3.0043	3.000	3.00183
F	0.07		0.04	0.03	0.07	0.02	0.19	0.23	0.02	0.07

(Fig. 4b). No evidence of correlation between δ (ppm) peak position of ^{1}H MAS NMR and total iron content was observed in this study.

3.2.3. 19F

The ^{19}F MAS-NMR spectra show only one resonance around –176 ppm, with similar SSB and FWHH evolutions (intensity and asymmetry) to those observed on ^{1}H spectra (Fig. 5a). Note that spinning sideband intensity in these spectra is lower than that in ^{1}H spectra, for samples with similar Fe_2O_3 content. This specific feature might be attributable to the very low F contents of our talc samples (there are only few F environments compared to H environments in the structure).

As for the elements discussed so far, plotting the FWHH of ^{19}F MAS-NMR *vs.* total iron content shows a linear correlation, confirming the effect of iron cations on the broadening of the ^{19}F resonance peak (Fig. 5b). This correlation suggests a FWHH limit value for iron-free talc at around 0.5 ppm. Again, no correlation was observed between the δ peak position of ^{19}F spectra and total Fe_2O_3 content.

3.2.4. ^{27}Al

All spectra for this element show two intense resonance peaks around 9 ppm and 65 ppm, which can be attributed to $^{[6]}Al$ and $^{[4]}Al$, respectively (Sanz & Serratosa, 1984). However, note the absence of the 65 ppm and 9 ppm resonance peaks in samples 11 and 9, respectively, suggesting a single site distribution for aluminium (Fig. 6). Note also that sample 11 contains traces of a 1:1 Al phyllosilicate, in which Al is present only in the octahedral sheet. For this sample, we observed a poor correlation between FWHH and iron contents (FWHH is considered identical for the two resonances) (Fig. 6). Nonetheless, the correlation trend is similar to those observed for Si, H, and F. Samples with lower total iron contents displayed δ shifts toward higher values. A limit for δ position is reached for Fe_2O_3 contents around 1 wt % for the two resonances.

3.3. Iron cationic site influence on the multinuclear MAS-NMR spectra

Talc structural formulae were calculated by combining NIR, Mössbauer, and chemical microprobe analyses from Petit *et al.* (2004a and b) with the NMR data collected in the present study (Table 4). According to Mössbauer results, iron was allocated to 3 different sites: an octahedral site with two valence states (Fe^{2+} and Fe^{3+}) and a tetrahedral site containing only Fe^{3+}. The distinction between $^{[6]}Al$ and $^{[4]}Al$ was calculated from the ^{27}Al MAS-NMR spectra by measuring the surface area of the bands located at 9 ppm and 65 ppm, respectively.

Our results, in particular multinuclear MAS-NMR spectra for the elements Si, H, and F (Fig. 7a), reveal the real influence of iron substitution in the structure of talc. Note that, although we noted the influence of iron on Al MAS-NMR spectra, we chose not to carry this investigation further as we lacked the adequate data to account for the large variations of Al amounts in all sites.

4. Discussion

4.1. General information on MAS-NMR spectra of ^{29}Si, ^{27}Al, ^{1}H, and ^{19}F

It is well known that the presence of ferromagnetic impurities causes severe broadening and poor resolution of MAS-NMR spectra (Grimmer *et al.*, 1983; Oldfield *et al.*, 1983; Altaner *et al.*, 1987), and this at only 1 or 2 wt.% iron-oxide contents. In this study, we used natural talc samples that are entirely free of iron oxides, and in which iron is a structural component of talc. In addition, we used the variation of the total struc-

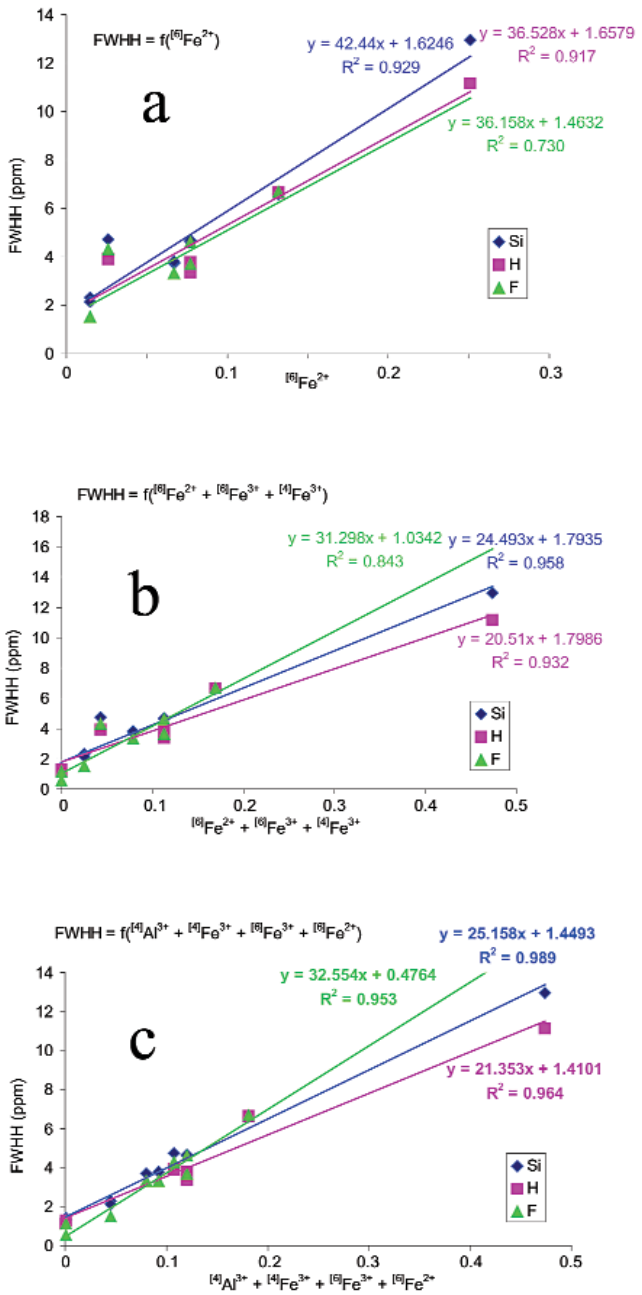

Fig. 7. (a) Correlations between FWHH of ^{29}Si, ^{1}H, ^{19}F MAS-NMR bands and $^{[6]}Fe^{2+}$; (b) Correlations between FWHH of ^{29}Si, ^{1}H, ^{19}F MAS-NMR bands and $\{^{[6]}Fe^{2+} + {}^{[6]}Fe^{3+} + {}^{[4]}Fe^{3+}\}$; (c) Correlations between FWHH of ^{29}Si, ^{1}H, ^{19}F MAS-NMR bands and $\{^{[6]}Fe^{2+} + {}^{[6]}Fe^{3+} + {}^{[4]}Fe^{3+} + {}^{[4]}Al^{3+}\}$.

tural iron content (0.04 to 2.07 oxide wt.% – principally Fe^{2+}) to understand the local crystal chemistry of various elements within the talc structure. The spectra that we obtained for the elements Si, Al, H and F show general characteristics that are encountered in all phyllosilicates (Lippmaa *et al*., 1980, 1981; Oldfield *et al*., 1983; Barron *et al*., 1985a and b; Herrero *et al*., 1985a and b; Huve *et al*., 1992; Welch *et al*., 1995; Alba *et al*., 2000; Di Leo & Cuadros, 2003). For instance, the ^{29}Si MAS-NMR spectrum of talc shows an asymmetrical peak around –98 ppm, attributed to Q^3 species (Lippmaa *et al*., 1980, 1981). In addition, the absence of Q^2 bands (due to very low tetrahedral substitutions) indicates a high degree of ordering around SiO_4 tetrahedron and thus the preservation of SiO_4 rings. This also insures a similar geometric environment for all OH groups or F atoms located within the hexagonal cavity. Another similarity is that ^{27}Al MAS-NMR spectra display almost systematically two resonances around 9 ppm and 64 ppm, corresponding to Al in octahedral and tetrahedral sites, respectively. The ^{1}H MAS-NMR spectra from our samples show a peak around 0.5 ppm, which is characteristic of structural hydrogen atoms located in the hexagonal cavity of trioctahedral phyllosilicates. Finally, the MAS-NMR spectrum of ^{19}F displays a single resonance around –176 ppm. For H and F atoms, the presence of only one peak and both position and intensity symmetry of the spinning sidebands indicate a single structural site with a bulk isotropic environment (OH-bond axes are perpendicular to the layers and point toward the hexagonal cavities, F replacing some OH groups). From these basic observations it is evident that a combination of MAS-NMR spectroscopy on Si, Al, H and F can provide important information about substitutions in tetrahedral and octahedral talc sites, and about the lack of important defects (absence of Q^2 bands for ^{29}Si, isotropic environment for H and F atoms).

4.2. Crystal chemistry of natural talc samples

Structural formulae are given in Table 4, calculated on the basis of electron- microprobe analyses (Table 1), infrared, Mössbauer and NMR results (Table 2). The $^{[4]}Al/^{[6]}Al$ ratios, which can only be obtained with MAS-NMR technique, permit to establish the accuracy of the structural formulae. The presence of two strong resonance peaks around 9 ppm and 65 ppm, attributed to $^{[6]}$Al and $^{[4]}$Al, respectively, indicates that Al can be distributed in both types of talc layers, as does Fe^{3+}. Chemical compositions indicate also that the deficiency in tetrahedral charges (due to replacement of Si by Al and Fe^{3+}) and the excess in octahedral charges (replacement of Mg by Al and Fe^{3+}) are compensated, resulting in a neutral talc structure. The location of Al and Fe^{3+} is due to the respect of this charge balance between tetrahedral and octahedral sites (Martin *et al*., 1999). Results on MAS-NMR spectra clearly indicate that Al location in the talc structure depends strongly on the geological environment present during the formation of a specific talc sample (work in progress), and that, in an extreme case, this can be responsible for the distribution of Al atoms in only one type of site, as was observed for samples 11 and 9 (Fig. 6). Our talc samples come from varied geological and geographic contexts and, as expected, every sample presents specific Si, H, and F MAS-NMR signatures, indicating a higher degree of variability in chemical composition and chemical substitution in talc than one would expect.

4.3. Influence of substitution in natural talc samples on NMR signals

Although observation of the distribution of Al between tetrahedral and octahedral site is a relatively easy task with this technique, the possible presence of iron in octahedral talc sheets cannot be detected directly with NMR spectroscopy. Indeed, the magnetic field homogeneity resulting from the interaction of *d* or *f* unpaired electrons in Fe^{2+} et Fe^{3+} atoms with the nucleus, classically induces a poor resolution on NMR spectra as well as NMR peak broadening (see above). However, because of the low total iron content in the talc sample studied (< 2% Fe_2O_3, exclusively in the talc structure), it is possible to obtain some information on structural iron (Fe^{2+} and Fe^{3+}) by investigating in detail the broadening of the NMR peaks. This peak broadening concerns ^{29}Si (Si located in tetrahedral sheet – Fig. 2a and 3b), ^{1}H and ^{19}F (located in hexagonal rings – Fig. 4a and b, 5a and b) and, to a lesser extend, ^{27}Al MAS-NMR peaks (Fig. 6). The linear dependence of the FWHH on total iron content for ^{29}Si, ^{1}H and ^{19}F confirms the effect of iron on the broadening of resonance peaks (Fig. 3b, 4b and 5b). We also noted that a FWHH limit value for pure iron-free talc is reached around 1ppm for the three elements considered. However, by taking into account the structural position of iron in talc, according to the structural formulae, , it is possible to show the influence of this element on multinuclear MAS-NMR Si, H, and F spectra (Fig. 7a).

Calculations by Palinko *et al*. (1996) indicate that the broadening of NMR peaks is influenced mostly by Fe^{2+}, due to the presence of more unpaired *d*-electrons in Fe^{2+} than in Fe^{3+}. Let's first consider the octahedral Fe^{2+} site, for which correlations between FWHH of Si, H and F MAS-NMR bands and the amount of $^{[6]}Fe^{2+}$ are shown in Fig. 7a. The correlation factors obtained using $^{[6]}Fe^{2+}$ are slightly lower than when using total iron contents (Fe_2O_3). If we now consider the sum of iron in the three sites concerned ($^{[6]}Fe^{2+} + {}^{[6]}Fe^{3+} + {}^{[4]}Fe^{3+}$), the correlation factor is again slightly lower than it would be doing the correlation with total iron content. Nonetheless, it is better than those obtained with only $^{[6]}Fe^{2+}$, indicating the possible presence of an additional effect that might influence the FWHH (Fig. 7b). Finally, the best correlations are found by introducing tetrahedral Al with the sum of $^{[6]}Fe^{2+} + {}^{[6]}Fe^{3+} + {}^{[4]}Fe^{3+}$. These correlations are even better than those obtained using total iron content alone, and stress the important effect of low tetrahedral substitutions on tetrahedral environment for at least Si, H and F NMR spectra (Fig. 7c). A similar conclusion was reached by Martin *et al*. (1996) using XAFS and FTIR spectroscopy, who showed the strong influence of Ge substitutions for tetrahedral Si in synthetic talc.

Another observation is that peak broadening resulting from increasing iron content is accompanied by a shift of the resonance peak position (δ). In our study, the ^{29}Si chemical shift occurred according to the Q^3 range, *i.e.*, between –90 ppm and –100 ppm, as predicted by Lippmaa *et al*. (1980 and 1981; see also Sanz & Serratosa, 1984). By analyzing Si/Al substitutions these authors concluded that the position of the shift is dictated by differences in composition of the octahedral sheet, as well as by the presence of second neighbours such as Al in the tetrahedral sheet. For all our NMR spectra, we could measure a resonance peak-position shift (δ), although for H, F and Al it is limited to high Fe_2O_3 contents, whereas it is constant for Si with decreasing Fe_2O_3 amounts, likely due to Fe_2O_3 influences. The limit value of δ for pure talc was found around –98.52 ppm for ^{29}Si. This value is not unlike that of all other trioctahedral phyllosilicates. Limit values obtained for ^{1}H and ^{19}F are around 0.5 ppm (sample 4) and –176 ppm (sample 9), respectively.

We conclude that our results on peak broadening and position shift (δ) obtained on NMR spectra can provide useful crystal-chemical data: for instance, one needs only measuring FWHH and δ position to evaluate the amount of cationic substitution in both tetrahedral and octahedral sheets ($^{[6]}Fe^{2+} + {}^{[6]}Fe^{3+} + {}^{[4]}Fe^{3+} + {}^{[4]}Al^{3+}$), with the sole exception of Ni-rich talc (Petit *et al.*, 2004a and b). The linear dependence of the FWHH *vs.* total iron content or, more precisely, *versus* the sum of $^{[6]}Fe^{2+} + {}^{[6]}Fe^{3+} + {}^{[4]}Fe^{3+} + {}^{[4]}Al^{3+}$ for all NMR elements, indicates iron cation dilution in the two talc sheets, but no Fe (or Al) cation segregation. These observations are in agreement with the data obtained by Martin *et al*. (1996) on tetrahedrally substituted synthetic talc (FTIR and XAFS data), as well as with those of Martin *et al*. (1999) and Petit *et al*. (2004a and b) on natural talc. Dilution, rather than clustering, of substituted cations in phyllosilicates is commonly a function of the conditions that prevailed during talc genesis (*i.e.*, high temperature and pressure).

5. Conclusions

Because of its beneficial properties to the final manufactured products, talc finds a wide variety of applications in paper coating, paint, ceramics, and polymer industries. However, because talc can exhibit a wide range of physical and chemical properties, it is necessary to accurately characterize its crystal chemistry in order to optimise its specific industrial applications. Indeed, heterovalent and homovalent substitutions in talc can give rise to quite variable characteristics, including modification of surface properties. This can influence the potential of epitaxial growth of polymers (Ferrage *et al*., 2002), as well as their hydrophobic properties (Bacchin *et al*., 2005) and lubricant properties (Martin *et al*., 2004). NMR spectroscopy, a very sensitive technique for Al-bearing minerals, was applied here to a number of natural talc samples containing low iron amounts. The results indicate clearly that very low iron amounts can be used as indirect NMR parameters to accurately characterize the crystal-chemistry of talc. An interesting application of this study is that, by simply measuring the bandwidth and peak position shift (δ) of MAS-NMR spectra of any of ^{29}Si, ^{1}H, or ^{19}F, one can obtain the precise content of even very small amounts of structural iron in talc.

Acknowledgements: We are grateful to the Luzenac Europe Company (in particular to Richard Baëza) for financial support to this study and to anonymous referees for the useful and constructive comments.

References

Alba, M.D., Becerro, A.I., Castro, M.A., Perdigon, A.C. (2000): High resolution ^{1}H MAS NMR spectra of 2:1 phyllosilicates. *Chem. Commun.*, **1**, 37-38.

—,—,—,— (2001): Hydrothermal reactivity of Lu-saturated smectites: Part II. A short range order study. *Am. Mineral.*, **86**, 124-131.

Altaner, S.P., Weiss, C.A., Kirkpatrick, R.J. (1987): Evidence from ^{29}Si NMR for the structure of mixed-layer illite/smectite clay minerals. *Nature*, **331**, 699-702.

Bacchin, P., Bonino, J.P., Martin, F., Combacau, M., Ferret, J. (2005): Surface pre-treatment of talc particles by CMC adsorption : study of adsorption and consequences on surface properties and settling velocity. *Colloids Surf. A: Physicochem. Eng. Asp.*, **272**, 211-219.

Barron, P.F., Slade, P., Frost, R.L. (1985a): Solid-state silicon-29 spin-lattice relaxation in several 2:1 phyllosilicates minerals. *J. Phys. Chem.*, **89**, 3305-3310.

—,—,— (1985b): Ordering of Aluminium in Tetrahedral Sites in Mixed-Layer 2:1 phyllosilicates by Solid State high-resolution NMR. *J. Phys. Chem.*, **89**, 3880-3885.

Bruni, S., Cariatti, F., Casu, M., Lai, A., Musinu, A., Piccaluga, G., Solinas, S. (1999): IR and NMR study of nanoparticle-support interactions in a Fe_2O_3-SiO_2 nanocomposite prepared by a sol-gel method. *Nanostructured Mat.*, **11**, 5, 573-586.

d'Espinose de la Caillerie, J.B., Man, P.P., Vicente, M.A., Lambert, J.F. (2002): ^{27}Al MQ-MAS NMR as a tool for structure determination in nanocomposite materials: the nature of Al pillars in "Al13-heidi" pillared clays. *J. Phys. Chem. B*, **106**, 4133-4138.

Cuadros, J., Sainz-Diaz, C., Ramirez, R., Hernandez-Laguna, A. (1999): Analysis of Fe segregation in the octahedral sheet of bentonitic illite-smectite by means of FT-IR, ^{27}Al MAS NMR and reverse Monte Carlo simulation. *Amer. J. Sci.*, **299**, 289-308.

Dékany, I., Turi, L., Fonseca, A., Nagy, J.B. (1999): The structure of acid treated sepiolites: small-angle X-ray scattering and multi MAS-NMR investigations. *Appl. Clay Sci.*, **14**, 141-160.

Di Leo, P. & Cuadros, J. (2003): ^{113}Cd, ^{1}H MAS NMR and FTIR analysis of Cd^{2+} adsorption on dioctahedral and trioctahedral smectite. *Clays Clay Miner.*, **51**, 4, 403-414.

Engelhardt, G. & Michel, D. (1987): High-Resolution Solid-State NMR of silicates and zeolites. John Wiley ed., ISBN 0471915971, 178 p.

Ferrage, E., Martin, F., Boudet, A., Petit, S., Fourty, F., Jouffret, F., Micoud, P., de Parseval, Ph., Salvi, S., Bourgerette, C., Ferret, J., Saint-Gérard, Y., Buratto, S., Fortuné, J.P. (2002): Talc as nucleating agent of polypropylene: morphology induced by lamellar particles addition and interface mineral-matrix modelization. *J. Mater. Sci.*, **37**, 1561-1573.

Fyfe, C.A., Brouwer, D.H., Lewis, A.R., Chezeau, J.M. (2001): Location of the fluoride ion in tetrapropylammonium fluoride silicalite-1 determined by ^{1}H/^{19}F/^{29}Si triple resonance CP, REDOR, and TEDOR NMR experiments. *J. Am. Chem. Soc.*, **123**, 6882-6891.

Galan-Huertos, E. & Rodas, M. (1973): Contribución al estudio mineralógico de los depósitos de Talco de Puebla de Lillo (León, España). *Boletín Geológico y Minero*, **84**, 347-365.

Gonzalez, A., de Saja, J.A., Alonso, J. (1995): Morphology and tensile properties of compression-moulded talc-filled polypropylene. *Mater., Plastics, Rubber & Comp. Proc. & Appl.*, **24**, 131.

Grimmer, A.R., von Lampe, F., Mägi, M., Lippmaa, E. (1983): High resolution ^{29}Si NMR of solid silicates: influence of Fe^{2+} in olivines. *Z. Chem.*, **23**, 343-344.

Herrero, C.P. & Sanz, J. (1991): Short range order of the Si, Al distribution in layer silicates. *J. Phys. Chem. Solids*, **52**, 1129-1135.

Herrero, C.P., Sanz, J., Serratosa, J.M. (1985a): Si, Al distribution in micas: analysis by high resolution ^{29}Si NMR spectroscopy. *J. Phys. C- Solid State Phys.*, **18**, 13-22.

—,—,— (1985b): Tetrahedral cation ordering in layer silicates by ^{29}Si NMR spectroscopy. *Solid State Commun.*, **53**, 151-154.

Herrero, C.P., Gregorkiewitz, M., Sanz, J., Serratosa, J.M. (1987): ^{29}Si MAS NMR spectroscopy of mica-type silicates: observed and predicted distribution of tetrahedral Al-Si. *Phys. Chem. Minerals.*, **15**, 84-90.

Huve, L., Delmotte, L., Martin, P., Le Dred, R., Baron, J., Saehr, D. (1992): ^{19}F MAS-NMR study of structural fluorine in some natural and synthetic 2:1 layer silicates. *Clays Clay Miner.*, **2**, 196-191.

Kentgens, A.P.M. (1997): A practical guide to solid-state NMR of half-integer quadrupolar nuclei with some applications to disorder systems. *Geoderma*, **80**, 271-306.

Kinsey, R.A., Kirkpatrick, R.J., Hower, J., Smith, K.A., Oldfield, E. (1985): High resolution aluminium-27 and silica-29 nuclear magnetic resonance spectroscopic study of layer silicates, including clay minerals. *Am. Mineral.*, **70**, 537-548.

Kirkpatrick, R.J. (1988): MAS NMR spectroscopy of minerals and glasses. *in* "Spectroscopic Methods in Mineralogy and Geology", F.C. Hawthorne ed. Mineralogical Society of America, Washington, DC, 70, 537-548.

Kulke, H. & Schreyer, W. (1973): Kyanite-talc schist from Sar a Sang, Afghanistan. *Earth Planet. Sci. Lett.*, **18**, 324-328.

Lausen, S.K., Lindgreen, H., Jakobsen, H.J., Nielsen, N.C. (1999): Solid-state ^{29}Si MAS NMR studies of illite and illite-smectite from shale. *Am. Mineral.*, **84**, 1433-1438.

Lippmaa, E., Mägi, M., Samoson, A., Engelhardt, G., Grimmer, A.R. (1980): Structural studies of silicates by solid-state high-resolution ^{29}Si NMR. *J. Am. Chem. Soc.*, **102**, 4889-4893.

Lippmaa, E., Mägi, M., Samoson, A., Tarmak, M., Engelhardt, G. (1981): Investigation of the structure studies of zeolites by solid-state high-resolution ^{29}Si NMR spectroscopy. *J. Am. Chem. Soc.*, **102**, 4889-4893.

Mägi M., Lippmaa, E., Samoson, A., Engelhardt, G., Grimmer, A.R. (1984): Solid-state high-resolution silicon-29 chemical shifts in silicates. *J. Phys. Chem.*, **88**, 1518-1522.

Martin, F., Ildefonse, Ph., Hazemann, J.L., Petit, S., Grauby, O., Decarreau A. (1996): X-ray absorption fine structure and Fourier transform Infrared studies of the Ge-Si-solid solution in talcs. *Eur. J. Mineral.*, **8**, 289-299.

Martin, F., Micoud, P., Delmotte, L., Maréchal, C., Le Dred, R., de Parseval, Ph., Mari, A., Fortuné, J.P., Salvi, S., Béziat, D., Grauby, O., Ferret, J. (1999): The structural formula of talc from the Trimouns deposit, Pyrénées, France. *Can. Mineral.*, **37**, 4, 975-984.

Martin, F., Bonino, J.P., Bacchin, P., Vaillant, S., Vautrin, W., Barthes, P., Ferrage, E. (2004): Composite material used like lubricant coatings. Patent PCT/FR03/03625.

Menczel, J. & Varga, J. (1983): Influence of nucleating agents on crystallization of polypropylene. I. Talc as nucleating agent. *J. Therm. Anal.*, **28**, 161-174.

Moine, B., Fortuné, J.P., Moreau, P, Viguier, F. (1989): Comparative mineralogy, geochemistry, and conditions of formation of two metasomatic talc and chlorite deposits: Trimouns (Pyrénées, France) and Rabenwald (Eastern Alps, Austria). *Econ. Geol.*, **84**, 1398-1416.

Morris, H.D., Bank, S., Ellis, P.D. (1990): ^{27}Al NMR spectroscopy of iron-bearing montmorillonite clays. *J. Phys. Chem.*, **94**, 3121-3129.

Oldfield, E., Kinsey, R.A., Smith, K.A., Nichols, J.A., Kirkpatrick, J. (1983): High-Resolution NMR of inorganic solids. Influence of magnetic centers on magic-angle sample-spinning lineshapes in some natural aluminosilicates. *J. Magn. Reson.*, **51**, 325-329.

Palinko, I., Lazar, K., Hannus, I., Kirisci, I. (1996): Step towards nanoscale Fe moieties: intercalation of simple and keggin-type iron-containing ions in-between the layers of Na-montmorillonite. *J. Phys. Chem. Solids*, **57**, 6-8, 1067-1072.

Petit, S., Martin, F., Wiewiora, A., de Parseval, Ph., Decarreau, A. (2004a): Crystal-chemistry of talc: a near infrared (NIR) spectroscopy study. *Am. Mineral.*, **89**, 319-326.

Petit, S., Decarreau, A., Martin, F., Buchet, R. (2004b): Refined relationship between the position of the fundamental OH stretching and their first overtones for clays. *Phys. Chem. Minerals*, **31**, 585-592.

Plévert, J., Okubo, T., Wada, Y., O'Keeffe, M., Tatsumi, T. (2001): Evidence of ^{29}Si NMR paramagnetic shifts in rare-earth zeolite LSX. *Chem. Commun.*, **20**, 2112-2113.

Purcell, E.M., Bloembergen, N., Pound, R.V. (1948): Relaxation effects in nuclear magnetic resonance absorption. *Phys. Rev.*, **73**, 679-712.

Rocha, J. & Pedrosa de Jesus, J.D. (1994): ^{27}Al satellite transition MAS-NMR spectroscopy of kaolinite. *Clay Miner*., **29**, 287-291.

Sainz-Diaz, C.I., Cuadros, J., Hernadez-Laguna, A. (2001): Analysis of cation distribution in the octahedral sheet of dioctahedral 2:1 phyllosilicates by using inverse Monte Carlo methods. *Phys. Chem. Minerals.*, **28**, 445-454.

Sanz, J. (1990): Distribution of ions in phyllosilicates by NMR spectroscopy. *in* "Spectroscopy in Mineralogy", A. Mottana & F. Burragato, eds. Elsevier, Amsterdam, 103-144.

Sanz, J. & Serratosa, J.M. (1984): ^{29}Si and ^{27}Al High-Resolution MAS-NMR spectra of phyllosilicates. *J. Am. Chem. Soc.*, **106**, 4790-4793.

Sanz, J. & Robert, J.L. (1992): Influence of structural factors on ^{29}Si and ^{27}Al chemical shifts of phyllosilicates 2:1. *Phys. Chem. Minerals.*, **19**, 39-45.

Schärer, U, de Parseval, Ph., Polvé, M, de Saint Blanquat, M. (1999): Formation of the Trimouns talc-chlorite deposit (Pyrénées) from persistent hydrothermal activity between 112 and 97 Ma. *Terra Nova*, **11**, 30-37.

Schroeder, P.A. (1993): A chemical, XRD and ^{27}Al NMR investigation of miocene Gulf Coast shales with application to understanding illite/smectite crystal-chemsitry. *Clays Clay Miner.*, **41**(6), 668-679.

Schroeder, P.A. & Pruett, R.J. (1996): Fe ordering in kaolinite: insights from ^{29}Si and ^{27}Al MAS NMR spectroscopy. *Am. Mineral*., **81**, 26-38.

Smith, K.A., Kirkpatrick, R.J., Oldfield, E., Henderson, D.M. (1983): High-resolution silicon-29 nuclear magnetic resonance spectroscopic study of rock forming silicates. *Am. Mineral.*, **68**, 1206-1215.

Tiganis, B.E., Shanks, R.A., Long, Y. (1996): Effects of processing on the microstructure, melting behavior and equilibrium melting temperature of polypropylene. *J. Appl. Polym. Sci.*, **59**, 663-671.

Welch, M.D., Barras, J., Klinowski, J. (1995): A multinuclear NMR study of clinochlore. *Am. Mineral.*, **80**, 441-447.

Received 30 September 2005
Modified version received 17 February 2006
Accepted 12 June 2006